The sentences that suggest that this paper proposes the idea mentioned in the assignment have been underlined
The rest of the listed papers do not discuss about the required topic.

TRANSIT LIGHT-CURVE SIGNATURES OF ARTIFICIAL OBJECTS

Luc F. A. Arnold
Observatoire de Haute-Provence, Centre National de la Recherche Scientifique, 04870
Saint-Michel-l'Observatoire, France; arnold@obs-hp.fr

ABSTRACT

The forthcoming space missions, able to detect Earth-like planets by the transit method, will a fortiori also be able to detect the transits of artificial planet-sized objects. Multiple artificial objects would produce light curves easily distinguishable from natural transits. If only one artificial object transits, detecting its artificial nature becomes more difficult. We discuss the case of three different objects (triangle, two-screen, and louver-like six-screen) and show that they have transit light curves distinguishable from the transits of natural planets, either spherical or oblate, although an ambiguity with the transit of a ringed planet exists in some cases. We show that transits, especially in the case of multiple artificial objects, could be used for the emission of attention-getting signals, with a sky coverage comparable to that of the laser pulse method. The large number of planets (several hundreds) expected to be discovered by the transit method by future space missions will allow us to test these ideas.

Subject headings: extraterrestrial intelligence — planetary systems

1. INTRODUCTION

Current Search for Extraterrestrial Intelligence (SETI) programs concentrate on the search for radio or optical laser pulse emissions (Tarter 2001). We propose here an alternative approach for a new SETI program: considering that artificial planet-sized bodies may exist around other stars and that such objects would always transit in front of their parent star for a given remote observer, we may thus have an opportunity to detect and even characterize them by the transit method, assuming that such transits would be distinguishable from a simple planetary transit. These objects could be planet-sized structures built by advanced civilizations, like very lightweight solar sails or giant very low density structures perhaps specially built for the purpose of interstellar communication by transit. The mass involved in these structures would be a negligible part of the mass of the mother planet. Such objects would remain much smaller than Dyson shells (Dyson 1960; Bradbury 2001), hypothetical artificial structures larger than the star itself.

Could the artificial nature of a planet-sized body be detected? If only one spherical body transits, there is, strictly speaking, an ambiguity on its nature—natural or artificial—although spectroscopy (or high angular resolution imaging in the future) could give significant insights to answer this question, like for HD 209458b (Vidal-Majar et al. 2003). But we know that a planetary transit light curve contains fine features due to the object's shape, which could be detected as soon as a 10^{-4} or better accuracy is reached for a Jupiter-sized object in front of a solar-type star. These features reveal planet oblateness (Barnes & Fortney 2003), double planets (Sartoretti & Schneider 1999), or ringed planets, which can also look oblate (Barnes & Fortney 2004). Although the sphere is the equilibrium shape preferred for massive and planet-sized bodies to adapt to their own gravity, one can consider nonspherical bodies, especially if they are small and lightweight and transit in front of a dwarf star to produce a detectable signal. Nonspherical artificial objects, like triangles or more exotic shapes, have each a specific transit light curve, as we show in this paper.

We also must consider the case of multiple objects: a remarkable light curve would be created by free-flyers transiting their star successively in a distinguishable manner. At each period, we would observe a series of transits whose number and timing would claim its artificial nature and a will to communicate.

We will be able to pay attention to these ideas with the coming space missions COROT (Bordé et al. 2003) and Kepler (Borucki et al. 2003), which will survey up to 6×10^4 and 10^5 stars, respectively, both reaching a photometric accuracy of $\approx 10^{-4} h^{-1/2}$, where h is the per point integration time in hours. The Kepler mission is expected to detect hundreds of planets (Borucki et al. 2003).

Tarter (2001) argued that an advanced-technology civilization trying to attract the attention of an emerging-technology civilization, such as we are, might do so by producing signals that would be detected within the course of normal astronomical exploration. The ongoing planetary transit search puts us exactly in the position of that emerging-technology civilization.

This paper discusses several simulated artificial transits (§ 2). Section 2.1 describes how we simulate transit light curves. In § 2.2, we point out the difficulty in detecting a compact artificial object from its transit light-curve shape, while other objects' light curves could display clearer features useful as attention-getting signals. Section 2.3 presents the possibility of multiple transits of artificial objects, which we consider as more clear attention-getting signals. In § 3, we first discuss the sky coverage of the transit-emitted signal, comparing it to the laser pulse method (§§ 3.1 and 3.2). We finally briefly present the implications that would arise from null or positive artificial transit detection by transit search programs (§ 3.3).

2. ANALYSIS OF SIMULATED ARTIFICIAL TRANSITS

2.1. Simulated Transits

The apparent stellar flux during the transit is evaluated from a simulated image of the star in which pixels are zeroed by the transiting object. The flux is normalized to the out-of-transit stellar flux. To have properly continuous stellar flux or planet-blocking flux functions (i.e., without steps due to pixelization when planet or star radii change), limb pixels are accurately interpolated. Stellar diameter is ≈ 800 pixels, and to save computer time, some integrals are computed only over a strip containing

Fig. 1.—Transiting objects: an equilateral triangular object (*top*) and the best-fit spherical planet and star (*bottom*) on the same scale. The star model for the triangle transit is HD 209458 with limb-darkening coefficients $u_1 + u_2 = 0.64$ and $u_1 - u_2 = -0.055$ (Brown et al. 2001). The triangle edge length is $0.280R_\star$. The object impact parameter is $b = 0.176$ (transit center). The best-fit sphere has an impact parameter of $b = 0.19$ and a radius of $r_p = 1.16R_J$. The best-fit star has $u_1 + u_2 = 0.66$, with $u_1 - u_2$ set to zero, and a nonsignificant radius increase of 0.5%.

the transit rather than over the whole stellar disk. The transiting object is assumed to have a circular orbit of radius $a = 1$ AU around HD 209458, a $1.15\,R_\odot$ star (Brown et al. 2001). The orbit projection onto the star is practically close to a straight line, although the code treats it as an arc of an ellipse. The impact parameter is computed for the transit center.

The nonplanetary object transit is fitted with a planetary transit using a Powell algorithm (Press et al. 1992) to minimize the square of the difference between both light curves. Four parameters in the fitting process are used: the stellar radius $R_\star$; the stellar limb-darkening coefficient $u_1 + u_2$, following Brown et al. (2001) and Barnes & Fortney (2003, 2004); the object impact parameter $b = |a \cos(i)|/R_\star$, where i is the inclination of the orbit with respect to projected orbit on the sky; and the object radius r_p. Two additional parameters, otherwise set to zero, are also considered for the fit when mentioned: the object oblateness f and the star limb-darkening coefficient $u_1 - u_2$, the latter being weakly constrained (Brown et al. 2001). One hundred sampling points were used for the fit, corresponding to a sampling time on the order of 5 minutes.

2.2. *A Single Object*

We now analyze the transit light-curve signature of three single nonplanetary objects. The first (a triangle) has a simple and compact shape, while the second and third (louver-like) have more elongated and complex structures. All have the same cross section, equal to a $r_p = 1.16R_J$ planet. The term R_J is defined as a Jupiter radius, $\approx 0.10\,R_\odot$.

The equilateral triangle is the regular convex polygon that differs most from the (planetary) circle. It is thus able to produce a priori a transit light curve different from a spherical body transit. We consider here an equilateral triangle with one side parallel to the transit direction (Fig. 1). This configuration generates a symmetrical light curve, which eliminates the possibility of transit of a nonzero-obliquity oblate or ringed object, which is known to produce an asymmetric light curve (Barnes & Fortney 2003, 2004).

Figure 2 shows that the triangle transit light curve cannot exactly be fitted by a spherical or an oblate body with $0°$ or $90°$ obliquity and that the fit residuals are symmetrical, suggesting a nonspherical, zero-obliquity, symmetrical transiting body. Our fit gives residuals that are on the order of 10^{-4}, within the photometric capabilities of $\approx 10^{-4} h^{-1/2}$ of space missions like *COROT* or *Kepler*. (Probably several transits should be cumulated to reach a sufficient accuracy.)

To produce a stronger signal, one can imagine these transiting objects in orbit around smaller (dwarf) stars. Moreover, as we point out in the § 1, arbitrary shapes rather than spherical ones would be more likely if the size of the object is smaller. Therefore, in order to produce a detectable signature with a small object, dwarf stars should be preferred by communicative civilizations. It must be noted that the curve in Figure 2 closely resembles the curve of a ringed planet transit as shown, for example, in Figure 1 in Barnes & Fortney (2004). This fitting degeneracy suggests that distinguishing a triangular object from a ringed planet would require a higher accuracy in the transit record than is mentioned here or in Barnes & Fortney (2004) to identify planetary rings.

If the nonspherical object rotates, the residual light curve will show an additional modulation due to object rotation in front of the background radiance gradient, i.e., the limb darkening of the star (J. Schneider 2004, private communication). This is verified in Figure 3. It shows the magnitude residuals from the light curve of a triangle making seven turns on itself perpendicular to the observer direction after subtraction of the best-fit sphere. At
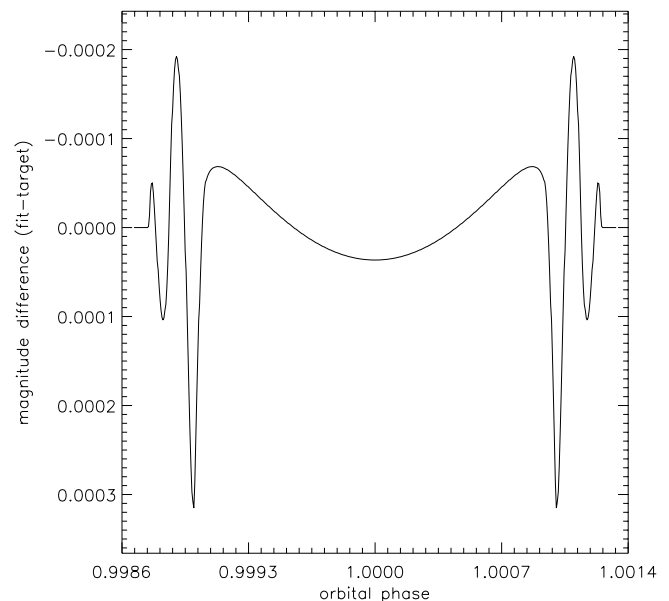

Fig. 2.—Magnitude difference between the transit of the triangular object and the best-fit sphere shown in Fig. 1. The fit of the object oblateness f either with $0°$ or $90°$ obliquity to maintain light-curve symmetry converges to solutions not significantly different from the case $f = 0$.
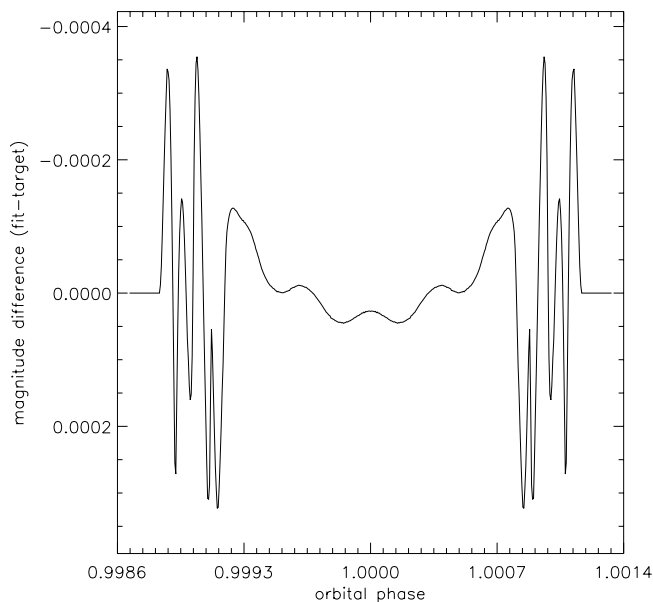
FIG. 3.—Magnitude difference between the transit of a rotating triangular object (same as shown in Fig. 1) and the best-fit spherical planet and star. The triangle makes seven turns on itself during the transit of HD 209458 at $b = 0.5$. The fit gives a transiting sphere of $1.17R_J$ at $b = 0.51$ and a star with $u_1 + u_2 = 0.67$, $u_1 - u_2 = 0$, and $R_\star$ increased by 1%. Here the curve is symmetric because the rotating object is in a symmetric position at transit center with respect to object orbital plane. If that were not the case, then the curve would be asymmetric.

FIG. 5.—Magnitude difference between the transit of a two-screen object (Fig. 4) and the best-fit spherical planet and star.

an impact parameter of $b = 0.5$, where the background gradient is larger around the transit center than at smaller b, the modulation outside ingress or egress is on the order of a few times 10^{-5} mag. But object rotation during ingress or egress significantly perturbs the light curve, which shows in our example several peaks of up to 6×10^{-4} mag with abrupt slope variations. The magnitude variation ultimately allows the measurement of the object apparent rotation period $p = P/k$, where P is the object rotation period and k the object rotational symmetry order.

Let us consider now a twofold object composed of two symmetrical screens (Fig. 4). If we neglect the structure linking the screens, the resulting transit can be considered as the sum of two identical light curves, slightly phase shifted, of a single compact convex body. Clearly, a sphere would only poorly fit the resulting light curve. This is verified in Figure 5, showing residuals 3 times larger peak-to-peak than those for the triangle, although both transiting objects have the same cross section. For a given impact parameter, the two-screen object ingress and
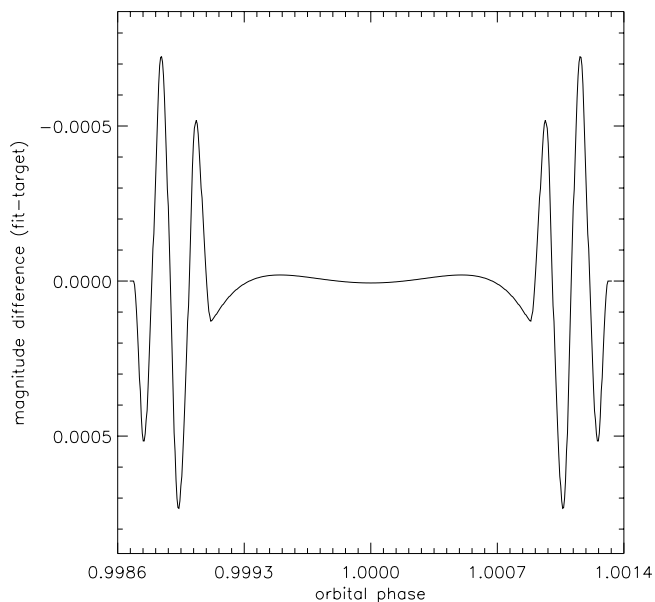
egress duration is longer than that for a compact object of similar cross section. Therefore, the fit by a sphere converges toward a larger impact parameter at which ingress and egress lengthen, and in order to maintain the overall transit duration and depth, planet and star radii are increased by $\approx$30%. Note that here again, the residuals' light curve shows an ambiguity with a ringed planet (Barnes & Fortney 2004).

The last example is a louver-like object, an elongated structure composed of six screens (Fig. 6). The screens produce undulating structures in the ingress and egress transit light curve that are visible in the residuals after best-fit sphere subtraction (Fig. 7). Here again, the object's elongated shape induces a longer ingress and egress than those for the previously considered objects: the fit converges toward a larger impact parameter, and planet and star radii are increased by $\approx$80% and $\approx$60%, respectively. The louver practically produces multiple transits. Each screen can indeed be considered as a single object transiting one after the other, like the two screens in the previous example. The detectability of the louver is twice as good as that for the triangle if we consider the peak-to-peak residuals, the cross section remaining the same. The oscillations during ingress and egress could be considered as an attention-getting

FIG. 4.—Transiting objects: a two-screen object (*top*) and the best-fit spherical planet and star (*bottom*) on the same scale. The fit gives a transiting sphere of $1.58R_J$ at $b = 0.51$ and a star with $u_1 + u_2 = 0.67$, $u_1 - u_2 = 0$, and $R_\star = 1.47\ R_\odot$.
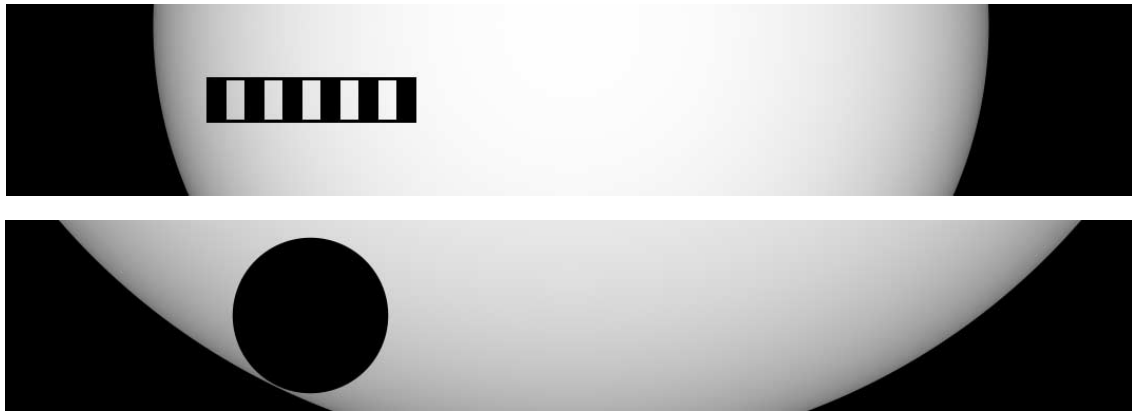
FIG. 6.—Transiting objects: a louver-like six-screen object (*top*) and the best-fit spherical planet and star (*bottom*) on the same scale. The fit gives a transiting sphere of $2.08R_J$ at $b = 0.79$ and a star with $u_1 + u_2 = 0.57$, $u_1 - u_2 = 0$, and $R_\star = 1.85\ R_\odot$.

signal from a communicative civilization, although the signal is in the 10^{-4} range (in our examples) and requires a sampling time on the order of 5 minutes. Detectability could even be higher, as we show in § 2.3 for multiple transits.

For the record, note also that a nonplanetary transit could be created by Dyson's sunflowers (Dyson 2003), hypothetical life forms spread into space to efficiently collect the energy of a distant star. These structures, if they exist, could be almost circular and quite compact, but also could look like sparse or dendritic arrangements. Nevertheless, large sunflowers would be far from the star, and transit probability consequently is very low.

2.3. *Multiple Objects*

Let us now consider a formation of several objects spatially arranged in groups to ingress the star in a remarkable manner, such as a series of prime numbers or powers of two. Even more remarkable would be a sudden swap between these two flying formations after several orbits. We consider that such multiple transits would clearly be attention-getting signals, and the will of communication would be obvious. The photometric accuracy required to detect 10^{-2} or deeper magnitude drops is reached
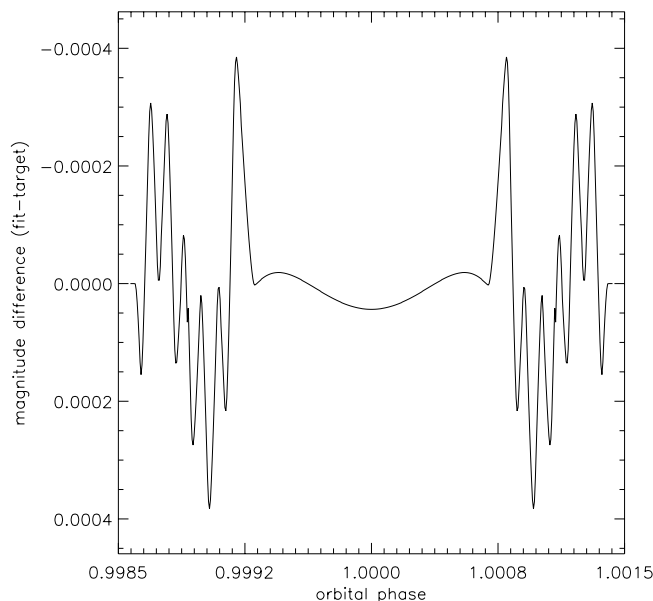
from the ground. Shallower light drops could be detected from space-based telescopes.

A minimal formation would be two objects, either identical or different so that the ratio of their cross sections would be remarkable, like integers, for example. The time between their respective ingress could also change after several identical transits, so their distance would change in a remarkable ratio, like integers again, for example.

If the objects transit individually, i.e., only one object in front of the star at a given moment, then we would have a series of identical drops in the light curve, which would look like a binary message (transit/no transit). If objects are closer to each other, they would transit quasi-simultaneously, and the depth of each drop would be proportional to the number of transiting objects in front of the star at a given time (Fig. 8). Assuming

FIG. 7.—Magnitude difference between the transit of a louver-like six-screen object (Fig. 6) and the best-fit spherical planet and star.
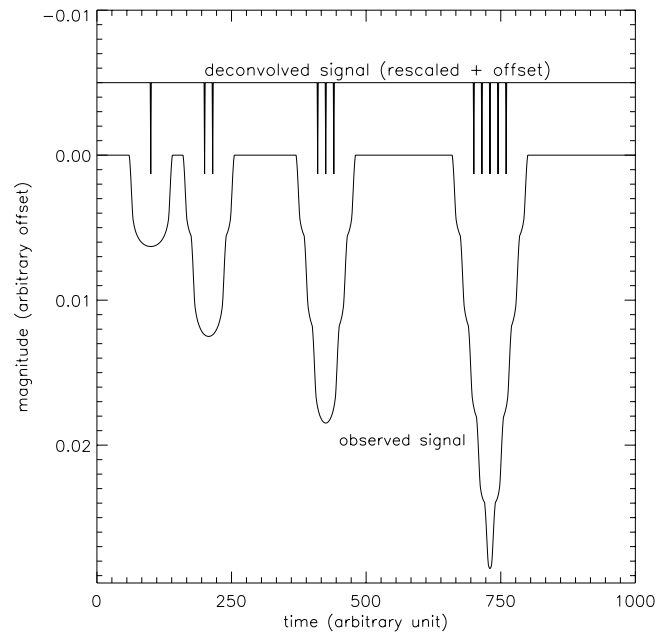

FIG. 8.—Example of multiple transits generated by 11 objects, grouped in prime numbers (1, 2, 3, and 5 objects). Note that the time between transits also increases as a prime numbers series. Each object has a Saturn-like cross section and transits the star HD 209458 with an impact parameter $b = 0.5$. Here due to the objects' size and space between them, only five objects could be simultaneously in front of the star for a given observer. The first transit of a single object allows deconvolution of the transits of multiple objects (*top curve*).

that all objects would be identical, a first single transit would give the key to deconvolve the transit light curve of one group, as also shown in Figure 8. The time *between the packets* could be used to introduce information in the message. In the figure, the time between each transit *inside a transit packet* is constant, but it could also be modulated to introduce more information inside one packet.

Such flying configurations would not necessarily be stable in their orbits and would require motors to stabilize the flying formation, unless objects are placed on the L4 and L5 Lagrange points respective to a more massive body, e.g., the mother planet. Due to the relative size of an object with respect to the star, only a limited number of objects could be in front of the star at a given time (five in our example), but this number could be larger in the case of Earth-sized objects, giving more degrees of freedom for information transmission, with the drawback of requiring better photometric sensitivity to be seen.

Compared to a single transit of an artificial object (triangular, for example, as discussed in § 2.2), a relaxed photometric accuracy would be required to detect the artificial nature of the multiple transits. It is likely that a civilization would rather build a series of (small) objects to generate multiple transits rather than a (large) single nonspherical object for communicative purposes.

3. DISCUSSION

3.1. *Directionality and Sky Coverage of the Transit Signal*

Is the transit method efficient for stellar communication compared to communication with laser pulses (Kingsley 2001)? Let us consider that one transit corresponds to one bit of information. Considering a solar-type star, the period of the transit signal is $T = a^{3/2}$. This signal is also observable over a solid angle of $\Omega = 4\pi R_\star/a$ from which the transit is visible during one period. (We neglect the object size with respect to $R_\star$.) We define the mean spatial data rate b_t by the number n of bits emitted over a given solid angle per second of time. The higher this quantity, the higher the method relevance for the emission of attention-getting signals. Taking into account that 1 yr is 3.2×10^7 s, we have

$$b_t = \frac{n\Omega}{T} = \frac{4\pi R_\star}{3.2 \times 10^7 a^{5/2}} \approx 2 \times 10^{-9} \text{ bits sr s}^{-1} \quad (1)$$

for an object in an Earth-like orbit ($a = 1$). It is increased by a factor of 10 if the object is at $a = 0.4$. Another factor of 10 is obtained with $n = 10$ transiting objects. The value of b_t could thus reach

$$b_t = \frac{n\Omega}{T} = \frac{10(4\pi)R_\star}{3.2 \times 10^7 (0.4^{5/2})} \approx 2 \times 10^{-7} \text{ bits sr s}^{-1}. \quad (2)$$

Precessing objects in a polar orbit would send the transit signal over 4π steradians (sr) but only after several periods.

For comparison, let us now consider the data rate from laser pulses, b_p. Kingsley (2001) calculated that up to 10^6 solar-type stars within a radius of 300 pc could be reached by 1 ns laser pulses of 10^{18} W peak power. The farthest target, on the signal reception side, would yet collect a few thousands of photons per pulse with a 10 m telescope. On the signal emission side, a visible laser beam produced by a 10 m telescope has a width of $0\farcs01$, covering a solid angle of $\Omega \approx 2 \times 10^{-15}$ sr. Assuming a laser duty cycle t of 1 s, equivalent to a laser mean power of 10^9 W following Kingsley (2001), we have

$$b_p = \frac{n\Omega}{t} \approx 2 \times 10^{-15} \text{ bits sr s}^{-1}. \quad (3)$$

Here b_p is much smaller than b_t. Nevertheless, one can argue, assuming that life is concentrated near stars only, that the emission of laser pulses elsewhere than toward stars would be ineffective and useless. Let us assume that an angle of $0\farcs1$ is shot around each star, corresponding to 30 AU for a star at 300 pc. With a 10 m emitting telescope and a beam width of $0\farcs01$, the $0\farcs1$ patch on the sky will require 100 s of time to be shot with the same laser duty cycle as above. Thus, the 10^6 solar-type stars considered by Kingsley (2001) would be equivalent to a complete sky coverage (4π sr), and b_p becomes

$$b_p = \frac{n\Omega}{t} \approx \frac{4\pi}{(10^6)(10^2)} \approx 1.3 \times 10^{-7} \text{ bits sr s}^{-1}. \quad (4)$$

We must note that the narrow angle of $0\farcs1$ considered above assumes that an extraterrestrial intelligence (ETI) civilization would have an excellent knowledge of the proper motion and distance of each of its targets in order to shoot the laser toward the correct patch of sky that anticipates the star motion during the laser propagating time. Otherwise, the narrow laser beacon would miss its target. Without this astrometric knowledge, an ETI civilization would have to shoot in a much larger patch of sky around each target: the statistical distribution of stars' proper motion measured with the *High-Precision Parallax Collecting Satellite* (*Hipparcos*) (F. Mignard 2005, private communication) within 300 pc is $0\farcs005$–$0\farcs01$ yr^{-1}. A star at 300 pc $\approx$ 1000 lt-yr typically will move by $\approx 5''$, which would be the typical patch of sky to be shot around a target star. Again with a laser beam width of $0\farcs01$, each target star would require on the order of 2.5×10^5 s $\approx$ 3 days emitting time, and the method would fall in the $b_p \approx 10^{-13}$ bits sr s^{-1} range. Of course a smaller emitting telescope could easily produce a wider beacon. But for a given pulse energy, the photon flux at the target would be smaller proportionally to the telescope's aperture ratio squared.

The values of b_p and b_t above show that both might reach the 10^{-7} bit sr s^{-1} level, although, as Kingsley (2001) wrote in his analysis, there is a lot of room to "play" with the numbers here. We consider that the sky coverage of both the laser and the transit methods have a similar efficiency in terms of data rate over a given solid angle.

3.2. *Other Aspects of the Comparison of Transits with Laser Beacons*

Section 3.1 shows that transits seem reasonably suited for the emission of attention-getting signals, as laser beacons are. We leave it to the reader to decide whether a 10^{18} W peak power laser or an Earth- or Jupiter-sized screen would be easier to build.

The world's most powerful lasers now under construction, like the Laser Megajoule (LMJ) in France[1] (André 1999; Cavailler et al. 2004) or the National Ignition Facility (NIF) in the US[2] (Miller et al. 2004), will produce pulses of 1.8×10^6 J within a few times 10^{-9} s, reaching instant power of up to 6×10^{14} W. This remains at least 1000 times weaker than the pulses invoked by Kingsley (2001). The LMJ would only allow up to 600 shots each year (given constraints on components' cooling, maintenance like optical alignment, and optics aging), including only 30 at full power (André 1999; Cavailler et al. 2004). This is far below the $\approx 10^7$ shots (1 Hz) required each year to reach the previously discussed b_p values. Thus, human technology with the LMJ or NIF will only allow b_p in the $\approx 10^{-13}$ bits sr s^{-1} range.

---

[1] See http://www-lmj.cea.fr/.
[2] See http://www.llnl.gov/nif/.

On the large screens side, the *Znamya-2* Russian experiment in 1993 successfully deployed a 20 m membrane in space (McInnes 1999). The program's future developments had considered structures up to 200 m, but it was stopped in 1999. It can nevertheless be considered as the very first step toward deploying large structures in space, although the object's cross section is yet far (10^{-11} to 10^{-13} times) from Earth- or Jupiter-sized objects. Current human technology clearly has $b_t = 0$.

Our definitions of b_p and b_t do not take into account the maximum distance at which these communicative methods remain efficient. For transits, 10^{-2} drops are detectable on faint and distant stars, for example, in the case of the $I = 15.72$ mag star OGLE-TR 132 discovered with a 1.3 m telescope (Bouchy et al. 2004; Moutou et al. 2004). But it is unlikely that the Optical Gravitational Lensing Experiment (OGLE) telescope would be able to discover transits of significantly fainter stars. OGLE-TR 132 lies at ≈ 2500 pc. A 550 nm, 10^{18} W laser pulse emitted from there with a 10 m telescope would yet result in a ≈ 100 photon bunch in a similar Earth-based telescope. The star itself gives ≈ 1000 photons nm^{-1} s^{-1}, meaning that with a time resolution better than 0.1 s and a spectral resolution of 1 nm, or simply with a time resolution better than 0.001 s and a broadband 100 nm *V* filter, the laser would still outshine the star. A 1.3 m telescope would only collect 2 photons pulse^{-1}, but detection remains possible at this flux level (Blair & Zadnik 2002) with a cooled photomultiplier and adequate time resolution. Therefore, in very first approximation, and leaving aside the knowledge required about target proper motion mentioned above, both methods may have quite similar ranges.

Transits of opaque objects would be achromatic (although one may imagine some spectroscopic coding) and thus detectable over the entire spectrum with a simple CCD, while the detection of 10^{-9} s pulses would require a more dedicated focal instrument. These arguments emphasize the relevance of artificial transits for stellar communication with respect to laser pulses.

Assuming a civilization controlling both lasers and planet-sized artificial structures, it is likely that if transits were used for the emission of attention-getting signals, laser pulses would be used for the emission of large amount of data *in a given direction, i.e., toward a given target*, because the data rate *per steradian* could easily be much larger with a laser than with the transit method.

3.3. *Implications of Artificial Transit Search Results*

Let us consider the implications of null results. Among all known variables stars, about 15×10^3 are eclipsing binaries, but none are known to have light curves that suggest artificial eclipsing objects. No Dyson shells have been identified up to

now (Bradbury 2001), although possible candidates exist, i.e., stars with an infrared excess.[3] These negative observations suggest that civilizations able to build star-sized structures simply do not exist. But it is possible to propose alternative explanations that do not preclude the existence of such civilizations, following and adapting the arguments of Blair & Zadnik (2002), for example, by invoking the incompleteness of the search in terms of sensitivity or targets. The detection of zero artificial transits by the end of the *COROT* and *Kepler* missions would also imply the same conclusions.

A positive result would, among other things, obviously motivate other planetary transit search programs. If upcoming space missions detect one artificial transit among 1000 new planetary transits, we reasonably could assume a mean value of one communicative civilization for 1000 planetary systems. If this mean value is true, the Poisson law gives a probability of 37% of detecting another communicative civilization within another sample of 1000 new discovered transits.

4. CONCLUSIONS

We have shown that detecting an artificial object from its transit light-curve shape requires excellent photometric accuracy. In our examples of transiting objects with Jupiter-like cross sections, the fit residuals are on the order of 10^{-4}. The residuals are not always distinguishable from the transit of a ringed planet. But during ingress and egress, louver-like objects produce flux periodic variations that could be attention-getting signals from a communicative civilization. It is more likely that a communicative civilization would privilege multiple transits inducing at least 10^{-3} or deeper light drops that are more easily identifiable as clear attention-getting signals.

Transits of artificial objects also could be a means for interstellar communication *from* Earth in the future. We therefore suggest to future human generations to have in mind, at the proper time, the potential of multiple Earth-sized artificial structures in orbit around our star to produce distinguishable and *intelligent* transits.

[3] See http://setiathome.ssl.berkeley.edu/~cconroy/ds.html.

REFERENCES

André, M. L. 1999, Fusion Eng. Design, 44, 43
Barnes, J. W., & Fortney, J. J. 2003, ApJ, 588, 545
———. 2004, ApJ, 616, 1193
Blair, D. G., & Zadnik, M. G. 2002, Astrobiology, 2, 305
Bordé, P., Rouan, D., & Léger, A. 2003, A&A, 405, 1137
Borucki, W. J., et al. 2003, in Towards Other Earths: *DARWIN/TPF* and the Search for Extrasolar Terrestrial Planets, ed. M. Fridlund & T. Henning (ESA SP-539; Noordwijk: ESA), 69
Bouchy, F., Pont, F., Santos, N. C., Melo, C., Mayor, M., Queloz, D., & Udry, S. 2004, A&A, 421, L13
Bradbury, R. J. 2001, Proc. SPIE, 4273, 56
Brown, T. M., Charbonneau, D., Gilliland, R. L., Noyes, R. W., & Burrows, A. 2001, ApJ, 552, 699
Cavailler, C., Fleurot, N., Lonjaret, T., & Di-Nicola, J. M. 2004, Plasma Phys. Controlled Fusion, 46, B135

Dyson, F. J. 1960, Science, 131, 1667
———. 2003, Int. J. of Astrobiology, 2, 103
Kingsley, S. A. 2001, Proc. SPIE, 4273, 72
McInnes, C. R. 1999, Solar Sailing: Technology, Dynamics and Mission Applications, (London: Springer-Praxis)
Miller, G. H., Moses, E. I., & Wuest, C. R. 2004, Nucl. Fusion, 44, S228
Moutou, C., Pont, F., Bouchy, F., & Mayor, M. 2004, A&A, 424, L31
Press, W. H., Teukolsky, S. A., Vettering, W. T., & Flannery, B. P. 1992, Numerical Recipes in C (2nd ed.; Cambridge: Cambridge Univ. Press)
Sartoretti, P., & Schneider, J. 1999, A&AS, 134, 553
Tarter, J. 2001, ARA&A, 39, 511
Vidal-Major, A., Lecavalier des Etangs, A., Desert, J.-M., Ballester, G., Ferlet, R., Hebrard, G., & Mayor, M. 2003, Nature, 422, 143